

Photophysical Properties of Biologically Compatible CdSe Quantum Dot Structures

Jeremiah A. Kloepfer,[†] Stephen E. Bradforth,[‡] and Jay L. Nadeau^{*,†}

Jet Propulsion Laboratory, California Institute of Technology, Pasadena, California 91109, and Department of Chemistry, University of Southern California, Los Angeles, California 90089

Received: November 29, 2004; In Final Form: March 28, 2005

The photophysical properties of CdSe and ZnS(CdSe) semiconductor quantum dots in nonpolar and aqueous solutions were examined with steady-state (absorption and emission) and time-resolved (time-correlated single-photon-counting) spectroscopy. The CdSe structures were prepared from a single CdSe synthesis, a portion of which were ZnS-capped, thus any differences observed in the spectral behavior between the two preparations were due to changes in the molecular shell. Quantum dots in nonpolar solvents were surrounded with a trioctylphosphine oxide (TOPO) coating from the initial synthesis solution. ZnS-capped CdSe were initially brighter than bare uncapped CdSe and had overall faster emission decays. The dynamics did not vary when the solvent was changed from hexane to dichloromethane; however, replacement of the TOPO cap by pyridine affected CdSe but not ZnS(CdSe). CdSe was then solubilized in water with mercapto-acetic acid or dihydrolipoic acid, whereas ZnS(CdSe) could be solubilized only with dihydrolipoic acid. Both solubilization agents quenched the nanocrystal emission, though with CdSe the quenching was nearly complete. Additional quenching of the remaining emission was observed when the redox-active molecule adenine was conjugated to the water-soluble CdSe but was not seen with ZnS(CdSe). The emission of aqueous CdSe could be enhanced under prolonged exposure to room light and resulted in a substantial increase of the emission lifetimes; however, the enhancement occurred concurrently with precipitation of the nanocrystals, which was possibly caused by photocatalytic destruction of the mercaptoacetic acid coating. These results are the first presented on aqueous CdSe quantum dot structures and are presented in the context of designing better, more stable biological probes.

Introduction

Much current research on CdSe semiconductor nanocrystals (quantum dots) is focused on understanding their behavior in liquid environments. This is due to their potential applications as luminescent biological labels and advanced sensors that utilize energy and electron transfer.^{1–5} CdSe quantum dots offer advantages over traditional fluorescent molecules because of their size-tunable emission at visible wavelengths, narrow emission spectra, and broad absorption spectra. However, CdSe nanocrystals do present several technical challenges toward their use in an aqueous, and hence biological, environment. Among them are their size, surface chemistry, and insolubility in water. In this article, we examine the photophysical properties of some common CdSe quantum dot structures before and after water solubilization, using steady-state and time-resolved spectroscopy. Our goal is to evaluate their use for the construction of advanced biological probes.

The standard procedure for synthesizing CdSe nanocrystals yields particles that range from 3 to 10 nm in diameter and are insoluble in aqueous solutions.⁶ They are coated with trioctylphosphine (TOP) and trioctylphosphine oxide (TOPO), of which the latter primarily coordinates to surface Se atoms;⁷ a simple schematic is shown in Figure 1. Excitation of CdSe nanocrystals promotes an electron from the valence to conduc-

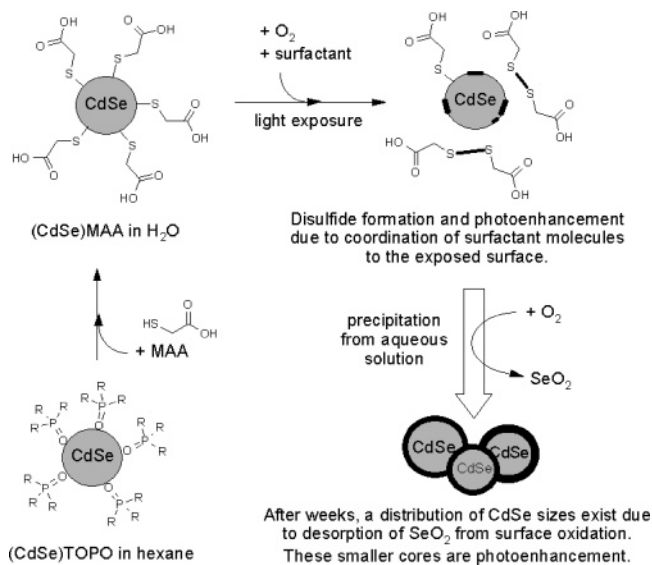


Figure 1. Schematic of some of the relevant CdSe quantum dot structures discussed in this article. Shown are the freshly synthesized trioctylphosphine oxide (TOPO)-coated CdSe's in a nonpolar solvent, water solubilization with mercaptoacetic acid (MAA), and then the decay of the aqueous structures leading to precipitation, photoenhancement, and surface oxidation. R = CH₂(CH₂)₆CH₃.

* To whom correspondence should be addressed. Current address: Department of Biomedical Engineering, McGill University, 3775 University Street, Montreal QC, Canada H3A 2B4. E-mail: jay.nadeau@mcgill.ca. Phone: 514-398-8372. Fax: 514-398-7461.

[†] California Institute of Technology.

[‡] University of Southern California.

tion band, which can then undergo radiative relaxation.⁸ Uncoordinated surface atoms give rise to trap states that lie within the band gap and reduce the quantum yield by providing alternative pathways of excited-state relaxation.

The interaction of the CdSe nanocrystal with its environment plays a crucial role in determining its luminescent properties. Passivating the surface traps with primary amines, polymer coatings, or higher band gap semiconductors (such as ZnS) increases the quantum yield.^{9–11} Other molecules may quench or enhance the emission through electron transfer with the quantum dots or through dipole–dipole processes such as fluorescence resonance energy transfer (FRET).^{2,12–14} The surface may also undergo physical modification and destruction as the samples age (Figure 1). Oxygen attacks exposed Se sites, resulting in the desorption of SeO₂ and a reduction in the nanocrystal diameter with a concurrent shift of the emission spectrum to the UV.⁷ Finally, the phenomenon of photoenhancement is observed in alcoholic solvents and refers to an increase in the luminescence quantum yield of CdSe nanocrystals as they are continuously exposed to light over several hours.^{15–17} The exact mechanism of this process remains controversial and has been variously suggested to result from passivation by SeO₂^{18,19} or interaction with water molecules.¹⁵

Commercial CdSe quantum dots are generally passivated with ZnS and then coated with a polymer layer that improves their quantum yield, solubility, and shelf life. This procedure is ideal for constructing simple fluorescent labels but can double the nanocrystal diameter and make the CdSe core less accessible to any application that would take advantage of electron and/or energy-transfer processes. Size is an important consideration in biological applications, where the transport of fluorescent labels across cell walls, cell membranes, and/or nuclear pores may be desired. In bacteria, nonspecific cell wall pore sizes measure up to 2 nm,²⁰ and pores for specific transport, up to 6 nm.²¹ In mammalian cells, the nuclear pore measures ~25 nm.²² Likewise, quantum dot core accessibility is required to regulate the luminescence in the presence of specific molecules or metabolic processes.

Standard methods for water-solubilizing bare CdSe quantum dots involve conjugating them to polar molecules containing thiol groups^{1,23} or embedding them in the nonpolar region of lipid micelles or vesicles.^{24,25} Commonly used thiol compounds are mercaptoacetic acid (MAA) and dihydrolipoic acid (DHLA). A CdSe synthesis method in water involving mercapto-alcohols and acids has even been developed,²⁶ as well as one method using sodium citrate.²⁷ Unfortunately, thiol compounds are notorious for their quenching of nanocrystal emission and precipitation under continuous light exposure.²⁸ They do, however, preserve the initial nanocrystal size and provide an intermediate to which other molecules, such as proteins and nucleic acids, can be attached.

In this article, the luminescence of CdSe structures and their ZnS-capped counterparts, referred to as ZnS(CdSe), is compared in a variety of solvents. TOPO-capped nanocrystals are suspended in a nonpolar solvent (hexane or dichloromethane). The TOPO is then replaced with pyridine, and the dynamics are studied in the same solvents. The particles are then solubilized with MAA and/or DHLA and studied in aqueous solvents (water and phosphate-buffered saline). Finally, the effects of both surface oxidation and photoenhancement are considered in water. Although previous studies have used steady-state and time-resolved spectroscopy to focus on the physical chemistry of a particular quantum dot structure, the work cataloged here is one of the first to compare the changes in emission of the same CdSe core as the surrounding coating and solvent are varied. Of particular interest to our research program is how the photophysics vary in the aqueous environments, with the hope that such knowledge will enable us to construct more

advanced quantum dot biological probes. The nomenclature (CdSe)X is used throughout this paper and denotes that X is the predominant outer coating of the CdSe core.

Experimental Section

Details of the CdSe synthesis have been previously published.^{5,29} Very simply, a modified technique was used where a cadmium salt replaces the standard organometallic precursor. Trioctylphosphine selenide (TOPSe) and cadmium acetate in a 1:1 concentration were injected into molten tech-grade TOPO (91%) at 305 °C and allowed to cool rapidly without the heating mantle. The resulting lemon yellow-colored quantum dots were washed in methanol and stored in hexane. A portion of this sample was ZnS-capped following standard techniques.^{9,10} A Zn/S precursor at 4 times the Cd/Se concentration was added dropwise over 15 min to the CdSe nanocrystals resuspended in TOP/TOPO at ~180 °C. The solution was baked at 90 °C overnight. The final ZnS-capped CdSe's were washed with methanol and stored in hexane. All syntheses were performed under nitrogen. To change the nonpolar solvent (between hexane and dichloromethane), QD solution was placed in a 50 mL round-bottom flask and subjected to rotary evaporation to remove 80–90% of the original solvent. The sludge was then taken up to the original volume in the new solvent; this procedure was repeated three to five times. To create pyridine-capped QDs, 5 mL of QD solution was subjected to rotary evaporation to remove >90% of the hexane. The sludge was redissolved in 5 mL of pyridine and stirred at 65 °C for 60 min. QDs were then precipitated with hexane and centrifuged to recover the pellet. The supernatant was decanted, and the solid was resuspended in pyridine. This process was repeated five to seven times.³⁰

CdSe was solubilized using mercaptoacetic acid (MAA), which replaces the TOPO coating allowing the quantum dots to be suspended in aqueous solution.^{23,28} Briefly, 0.48 mL of MAA was added to 2.5 mL of ~1 μ M TOPO-capped QDs in dichloromethane and rocked gently for 2 h in the dark. After the addition of 2.5 mL of phosphate-buffered saline (PBS: 6.5 mM Na₂HPO₄, 1.47 mM KH₂PO₄, 137 mM NaCl, 2.7 mM KCl, pH 7.5), the solution was vigorously agitated, and the layers were allowed to separate naturally. The pigmented layer was removed and washed two to three times in PBS by centrifugation (5 min at 14 000 rpm in a microcentrifuge) and removal of supernatant. Finally, the resulting colloid was suspended in 1–2 mL of PBS and dialyzed versus 2 L of PBS or ddH₂O for 2 h to remove residual MAA.

ZnS-capped CdSe structures were poorly solubilized with MAA and were thus solubilized with dihydrolipoic acid (DHLA).¹ The DHLA solubilization procedure for CdSe and (CdSe)ZnS was as follows: TOPO-capped QDs in dichloromethane were rotovapped to remove ~90% of the solvent. The particles were then suspended with a few drops of pyridine and methanol to displace the TOPO with pyridine and then mixed with DHLA suspended in methanol and ddH₂O. Tetramethylammonium hydroxide was added until the solution was basic (pH ~11), and the mixture was then maintained at 65 °C under nitrogen for several hours. After cooling, the QDs that were still suspended in the mixture were dialyzed for 2 h versus ddH₂O or PBS. The final pH of all water-soluble CdSe structures was approximately 7.

All solubilization procedures were performed in the dark. For tests of the effects of light exposure, QDs in a glass cuvette were exposed to a hand-held UV wand on the long-wavelength (365 nm) setting for a specified amount of time.

Cross-linking agent 1-ethyl-3-(3-dimethylaminopropyl)carbodiimide hydrochloride (EDC) is used to couple molecules with carboxylic acid groups to molecules containing primary amines by forming amide bonds³¹ and was used in these experiments to bond either of two very different biomolecules to the solubilized quantum dot structures. Adenine (6-aminopurine or 6AP) is a small molecule (MW 135) that is redox-active; it is the most readily oxidized DNA base after guanine and has been shown to modify the steady-state and time-resolved emission properties of CdS nanocrystals.³² The protein transferrin is a large (80 kD) glycoprotein without redox activity that is expected to act as a simple passivating agent on the QD surface. Its function is as an iron carrier, and we studied it in its iron-bound (holo) form.⁵ Conjugates were prepared as 1 mL reactions in PBS. For CdSe QDs, each reaction contained 1–2 mg of EDC, 0.1 mg of holotransferrin or 10 mM adenine, and 200 μ L of the solubilized QD solution at an approximate concentration of 1 μ M. For (CdSe)ZnS QDs, each reaction contained 1–2 mg of EDC, 0.01 mg of holotransferrin or 1 mM adenine, and 200 μ L of the solubilized QD solution at an approximate concentration of 100 nM. Conjugation was for 2 h in the dark, unless otherwise stated, and unbound conjugate was removed by dialysis or centrifugation and washing in dH₂O. The formation of amide bond linkages was confirmed by Fourier transform infrared spectroscopy (FTIR).

Emission lifetimes were recorded using the time-correlated single-photon-counting (TCSPC) technique. The new experimental setup is described as follows: samples were excited with laser pulses provided by the frequency-doubled output of a Ti:sapphire regenerative amplifier operating at a 200 kHz repetition rate. The peak pulse excitation wavelength was 400 nm unless otherwise noted, and the bandwidth was about 3 nm at full width at half-maximum (fwhm). The temporal width of the pulses was approximately 100 fs at fwhm assuming a Gaussian line shape. Laser pulses were focused into the sample using a 15 cm focal length lens because it was desirable to have sample excitation occur in a broad and regular focal volume to avoid nonlinear effects that might occur in a solvent if focusing was too tight. On average, the peak pulse intensity at the sample was 5×10^8 W/cm² after attenuation of the laser light with neutral density filters placed before the focusing lens.

Emission was collected perpendicular to the excitation beam with a 3.5 cm focal length lens and focused into a monochromator with a 10 cm focal length secondary lens. Both optics had a diameter of 1 in., and the focal length of the secondary lens was chosen on the basis of an *f* number of 3.9 for the monochromator. High and low band-pass filters, rejecting at least 90% of the light above 750 nm and below 450 nm, respectively, were placed before the monochromator entrance slit to discriminate against any stray laser light. The monochromator was a CVI CMSP112 double spectrograph with a $1/8$ m total path length in negative dispersive mode with a 1200 groove/mm grating. Typically, the slit widths were 0.6 mm and, on the basis of a monochromator dispersion of 8 nm/mm, provided 5 nm resolution. The PMT was mounted on the exit slit. The PMT was a Hamamatsu RU3809 microchannel plate detector powered by a variable high-voltage power supply. The usual operating voltage was -30 kV to maximize the time resolution of the detector.

Signals were amplified and then recorded with a Becker and Hickl SPC-630 photon-counting board. A small portion of the excitation beam was directed into a fast photodiode to provide

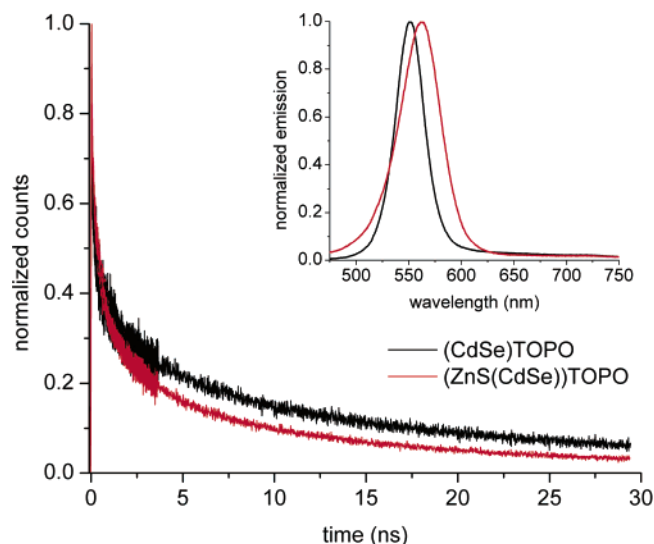


Figure 2. Emission of CdSe (black) and the corresponding ZnS-capped counterpart (red) as measured with the time-correlated single-photon-counting technique. The nanocrystals had a trioctyl phosphine oxide (TOPO) outer coating from the synthesis solution and were dissolved in hexane. (Inset) Normalized steady-state emission spectra of the same particles.

a reference signal. Typical discriminated count rates were held to 2000 counts/s or 1% of the laser repetition rate to avoid pulse pileup.

Samples were held in Spectrosil glass cuvettes purchased from Starna Cells with an internal path length of 1 cm. All solutions were stirred with a miniature stir bar and motor to prevent sample destruction and aggregation. Most sample concentrations were maintained below 1 μ M to minimize concentration effects such as light reabsorption; however, some of the aqueous quantum dot samples required a higher concentration because of their weak emission. It was confirmed that there was no change in the time-resolved emission as the concentration was varied. Quantum dot concentrations were estimated using published extinction coefficients.³³

Lifetime traces were analyzed with a modified version of a fitting program that utilizes the iterative deconvolution technique. The instrument response functions for the convolution were recorded from scattered light off of a dilute solution of coffee creamer. Typical fwhm values were ~ 37 ps. Emission measurements on fluorescent standards reproduced the published lifetimes: 12.7 ps for pinacyanol chloride in ethanol, 1.68 ns for rhodamine B in water, and 4.16 ns for the fluorescein dianion in 0.001 M NaOH.³⁴ Quantum yields were determined relative to the fluorescein dianion ($\sim 92\%$ in 0.1 N NaOH) with 450 nm excitation and using the Parker–Reas method. Steady-state emission spectra were measured inside the photon-counting setup with an Ocean Optics S2000 fiber-optic spectrometer. Outside the setup, some spectra were collected with a Hitachi F-4500 fluorimeter. Absorption spectra were collected on a Hewlett-Packard 8453 or a Cary 50 UV–visible spectrophotometer.

Results and Discussion

Emission of CdSe and ZnS(CdSe) in Nonpolar Solvents.

The results shown in this study were obtained from one synthesis of CdSe quantum dots, a portion of which were then ZnS-capped. Their normalized time-resolved and steady-state emission in hexane are displayed in Figure 2. Both samples were coated with TOP/TOPO. Peak emission for the bare CdSe

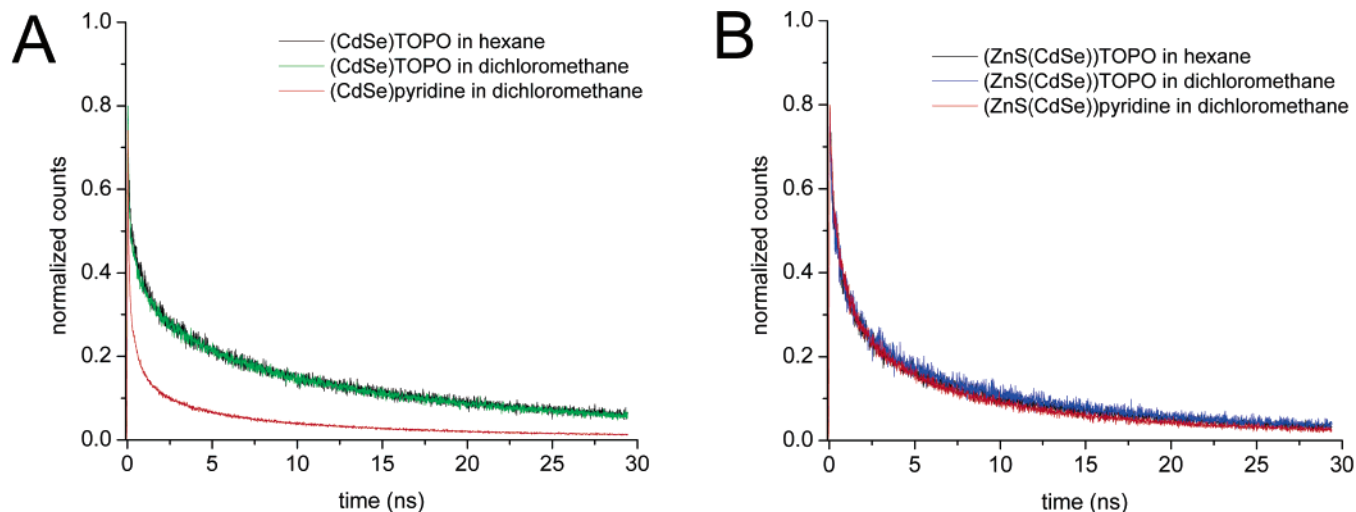


Figure 3. Effects of solvent and cap exchange in nonpolar solvents on the time-resolved emission. (A) TOPO-capped CdSe shows the same spectrum in hexane (black) as in dichloromethane (green); a significant loss of the slow component is seen when TOPO is replaced by pyridine (red). (B) Comparable spectra are seen with TOPO-capped ZnS(CdSe) in hexane (black) and in dichloromethane (blue) and with pyridine-capped ZnS(CdSe) in dichloromethane (red).

TABLE 1: Best-Fit Values for a Multiexponential Fit of the Data Shown in Figure 1^a

	A_1	τ_1 (ns)	A_2	τ_2 (ns)	A_3	τ_3 (ns)	A_4	τ_4 (ns)
CdSe	1.85	0.018	0.35	0.31	0.15	3.35	0.23	21.3
ZnS(CdSe)	1.85	0.018	0.47	0.31	0.25	3.35	0.13	21.3

^a These values were obtained after iterative reconvolution with the experimental instrument response function. Error bars are ± 0.05 for all amplitudes and the following for the time constants: τ_1 , ± 0.01 ; τ_2 and τ_3 , ± 0.05 ; and τ_4 , ± 0.1 .

quantum dots was centered at 550 nm. Upon ZnS capping, the peak wavelength shifted to 565 nm, and the spectrum was broadened. (ZnS(CdSe))TOPO had a larger short-time and smaller long-time decay than the uncapped samples. The decays are qualitatively similar to what was observed in the frequency domain measurements of Hines et al. comparing CdSe and ZnS(CdSe).¹⁰

No change in the decay curves was observed when the solvent sample was changed from hexane to dichloromethane. However, replacement of TOPO by pyridine led to a loss of the slow-decay component for CdSe (Figure 3A). This was accompanied by a complete quenching of fluorescence emission (not shown). No corresponding change was seen with ZnS(CdSe) (Figure 3B).

To date, no detailed physical mathematical model has been used to describe quantum dot emission dynamics. In previous studies, both exponential sums and stretched exponentials were used to simulate the lifetime decay of various quantum dot structures including CdSe, CdS, and GaSe, among others, with varying degrees of success.^{10,15,35–37} We fit the data in Figure 2 with a sum of exponential decays to give the reader some quantitative values for the time scales involved. A minimum of four exponential decays were required, and when convoluted with the instrument response function, the rise was instrument-limited. Interestingly, the same time constants could be used to fit both the uncapped and ZnS-capped CdSe data plotted in Figure 2, with variations in the preexponential amplitudes. The best-fit results are presented in Table 1. (The reduced χ^2 values are 1.15 and 1.09 for the CdSe and ZnS(CdSe) data, respectively.)

Uncapped CdSe Structures in H₂O after Solubilization and Conjugation. Solubilization with MAA and DHLA removes the TOP/TOPO coat and forms a sulfur–cadmium

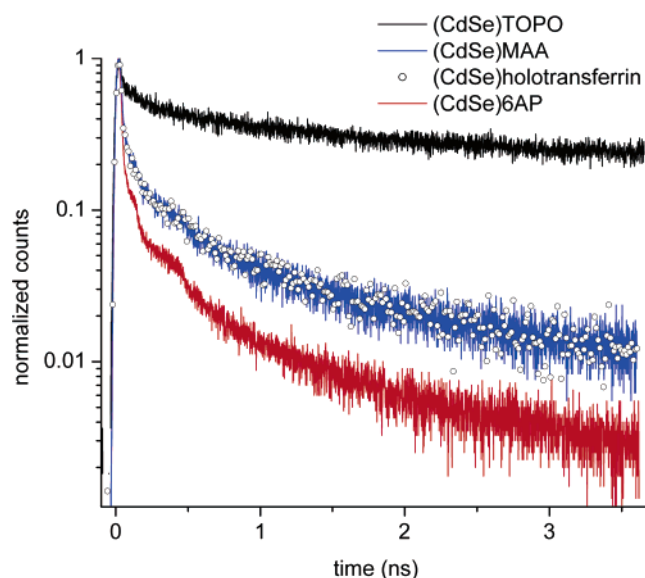


Figure 4. log-scale plot of the emission of CdSe in hexane ((CdSe)-TOPO, black), compared with several water-soluble versions. Cap exchange was used to remove the TOPO and suspend the CdSe in mercaptoacetic acid (MAA) (blue). This also provided a carboxylic acid backbone upon which the protein holotransferrin (O) and the nucleic acid adenine (6AP) (red) were attached.

bond at the quantum dot surface. Both (CdSe)MAA and (CdSe)-DHLA were stable in aqueous solutions over a period of weeks as long as they were stored in the dark; however, both of these thiol compounds quenched the CdSe emission. With DHLA, quenching was complete, and no steady-state or time-resolved emission could be collected. With MAA, the quantum yield was reduced to $\sim 0.01\%$ from $\sim 3\%$ for CdSe(TOPO) in hexane.

A comparison of the decay curves for (CdSe)MAA in water and (CdSe)TOPO in hexane is plotted in Figure 4, using a log scale for emphasis. There was nearly complete quenching of the nanosecond emission by MAA. The weak oscillations within 0.5 ns are completely accountable when the instrument response function is included. There was no difference in the decay when (CdSe)MAA was dissolved in phosphate-buffered saline (PBS) versus deionized water (not shown; available in Supporting Information Figure 1S). The data sets are normalized to peak counts equal to 1 to better illustrate the dynamic quenching.

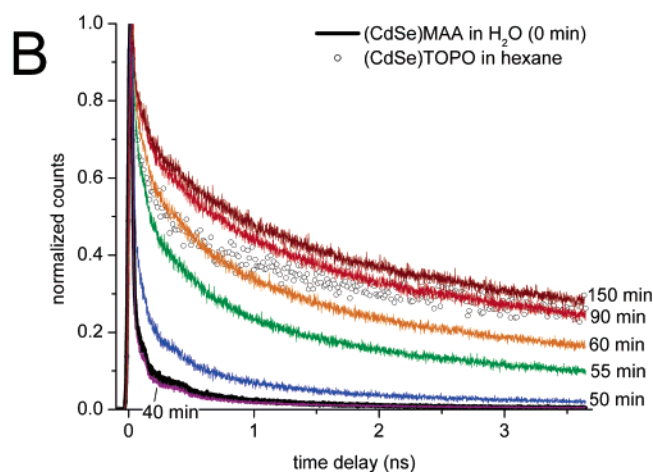
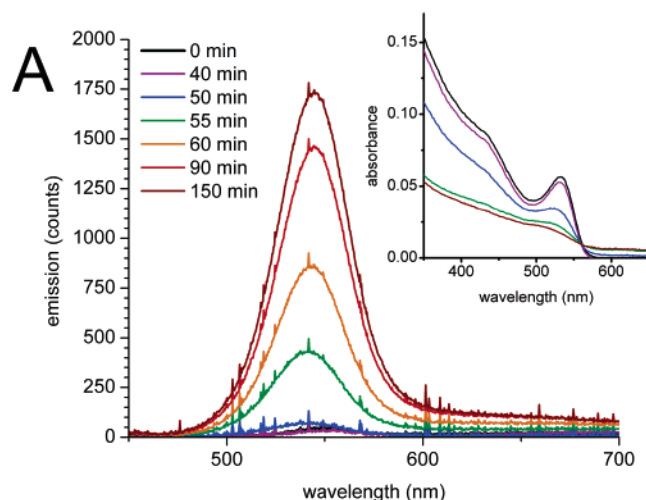


Figure 5. Photoenhancement of water-solubilized QDs exposed to near-UV light. (A) Steady emission of (CdSe)MAA after exposure to a UV lamp at several time intervals. Shown are the starting points after solubilization in the dark (black) and after light exposure for 40 min (violet), 50 min (blue), 55 min (green), 60 min (yellow), 90 min (red), and 150 min (maroon). (Inset) Absorption spectra at the starting point (black) and at 40, 50, 55, and 150 min. (B) Corresponding emission profiles at several time intervals, showing the starting points after solubilization in the dark (solid black) and after light exposure for 50 min (blue), 55 min (green), 60 min (yellow), 90 min (red), and 150 min (maroon). The time-resolved spectrum of TOPO-capped CdSe in hexane is included for comparison (○).

Although showing unnormalized data might offer insight into the amount of static quenching that occurs when quantum dots are solubilized, this comparison is difficult because the water-solubilized structures required a higher concentration, higher excitation energy, and longer data collection period than the nonpolar solvent forms to obtain useful data. If the assumption is made that the extinction coefficients of both forms are about equal, then the count rate from (CdSe)MAA is estimated to be at least 5 times lower than that from (CdSe)TOPO.

Also shown in Figure 4 is the time-resolved emission obtained from (CdSe)MAA structures conjugated to the nucleic base adenine (6AP) and the protein holotransferrin (HOLO) using the cross-linking agent EDC. The protein had no effect on the observed dynamics, whereas adenine provided additional quenching of the long-time emission.

Upon continuous exposure to room light or light from a UV lamp, (CdSe)MAA quantum dots began to precipitate but also experienced a concurrent increase in luminescent intensity. This photoenhancement effect is demonstrated in Figure 5 for (CdSe)MAA in PBS after continuous exposure to 365 nm light for increasing amounts of time. In Figure 5A, the changes in the steady-state emission and absorption spectra are plotted (inset). The corresponding decay curves are graphed in Figure 5B. After 40 min of continuous UV exposure, there were only slight changes in the steady-state spectra and emission decays. After 10 more minutes of exposure, there was a slight increase in emission intensity and longer time scale luminescence. The initial exciton peak in the absorption spectrum became less well defined, and the quantum dots began to visibly clump in the sample cuvette. The aggregated (CdSe)MAA remained suspended in solution only because the sample was stirred rapidly. Increasing intervals of UV exposure resulted in a complete loss of solubility and a smeared absorption profile but a dramatic enhancement in emission. The final steady-state emission spectrum shifted to the UV by 5 nm. The emission dynamics changed dramatically, with a long-time decay on par with the decay of the original TOPO-coated quantum dots in hexane.

Capped ZnS(CdSe) Structures in H₂O after Solubilization and Conjugation. ZnS-capped CdSe water-solubilized with MAA is notoriously unstable, even under dark conditions.¹ DHLA is somewhat better at suspending ZnS(CdSe) in water

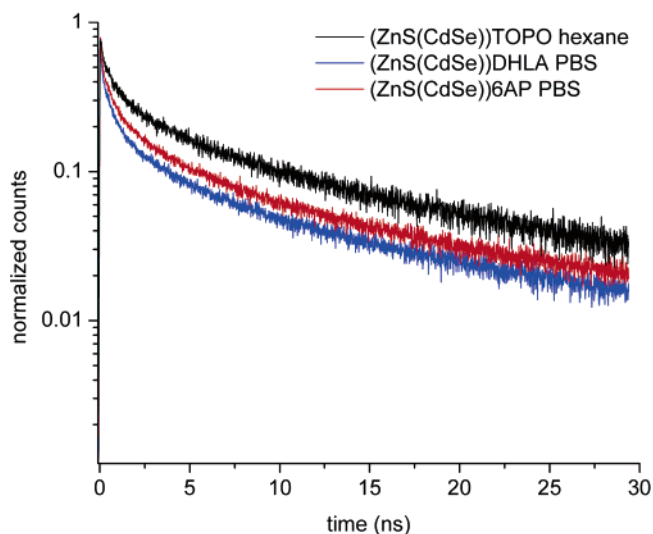


Figure 6. log-scale plot of the emission of TOPO-coated ZnS-capped CdSe (black) compared with its water-soluble counterparts. ZnS(CdSe) was suspended in PBS with dihydrolipoic acid (DHLA, blue), a portion of which was then conjugated to adenine (6AP, red).

and was used in this study. Shown in Figure 6 is the time-resolved emission of this solubilized structure alone, and after conjugation to adenine, versus the emission decay of ZnS(CdSe) in hexane. There was an overall quenching with the DHLA structure, though the change was not as intense compared to what was observed with bare CdSe quantum dots. There was no additional quenching when adenine was conjugated to (ZnS(CdSe))DHLA; rather, there may have been a slight enhancement of the emission.

Physical Mechanisms of Excited CdSe. Before discussing the results, it is useful to review the possible mechanisms of deactivation for photoexcited CdSe quantum dots, over which there is still some debate. Transient absorption³⁸ and fluorescence upconversion studies¹⁸ have been performed to explain the earliest time-scale dynamics. Bawendi et al. performed some of the earliest time-resolved emission studies over longer time scales.⁸ The electronic structure underlying the conduction band is complex and includes dark exciton states. Surface defects give rise to trap states that lie within the band gap and

complicate the dynamics. Excitation of CdSe (at 400 nm) promotes an electron high in the conduction band. Subsequent relaxation to the bottom of the conduction band is rapid, as evidenced by the instrument-limited rise times in the time-resolved data. The exciton emission arises from radiative relaxation of these electrons to the ground state and likely contributes to the fastest lifetime decays. Dark exciton states may contribute to processes that extend the emission lifetime. Alternatively, these conduction band electrons may localize in shallow trap states (i.e., trap states at or just below the bottom of the conduction band). From here, these electrons may repopulate the conduction band or thermalize into deeper trap states. In the former case, the lifetime is extended; the latter contributes to nonexciton emission or nonradiative mechanisms that lower the overall quantum yield. A combination of all of these processes along with differences between the individual nanocrystals in a population gives rise to highly multi- and/or stretched-exponential emission dynamics that occur over a nanosecond time scale and are observed in this experiment.

CdSe versus ZnS(CdSe) in Nonpolar Solvents. Previous work has shown that the quality of the quantum dot synthesis determines the shape of the time-resolved emission decay.³⁹ As the surface and lattice structure of the CdSe core is improved, the quantum yield increases to as high as 80%, and the decay profile becomes single exponential in character. It was therefore important that comparisons between the different capped and uncapped quantum dot structures were performed on the same CdSe batch. As the low quantum yield ($\sim 3\%$) and the decay profile in Figure 2 indicate, the quality of the synthesis in this study is low. This is probably due to using cadmium acetate as a precursor and is consistent with previously published results.⁴⁰ ZnS capping of an aliquot of this sample improves the luminescent intensity, but it is noted that as the bare CdSe samples age over the course of 6 months in the dark their luminescence intensity increases to match that of the ZnS-capped particles. The exact mechanism for this is unknown, but surface oxidation may play a role. Finally, the corresponding red shift and broadening of the steady-state emission spectrum of ZnS-(CdSe) is probably due to increased particle diameter and less heterogeneous size distribution.

ZnS capping has been suggested to enhance the quantum yield by reducing the population of dark dots, decreasing the blinking "off" time, or passivating the surface traps.^{9,10,15} The emissions in Figure 2 are consistent with the latter case because reducing the number of surface states would reduce the availability of alternative pathways that extend excited-state deactivation, leading to an overall faster decay as we observe. It is not likely that new pathways are created because the fit time constants in Table 1 do not change with ZnS capping. If ZnS stabilized shallow trap states and/or decreased the probability of moving to deep trap states, then the amplitude of the longest time constant would be expected to decrease while that of the shorter time constants increased in the simple exponential fit.

The emission of both CdSe and ZnS(CdSe) does not change when the nonpolar solvent is varied without removing TOPO, indicating that the electronic structure of the core is well preserved by the surrounding TOPO shell. The ability of pyridine to quench CdSe emission suggests electron transfer between the electron-donating amine and the Cd sites; this is consistent with what has been observed in steady-state spectra from amino-dendrimer conjugated QDs.³⁰ However, it has also been shown that certain primary amines (dodecylamine and allylamine) enhance emission in both CdSe and ZnS(CdSe), probably by passivating surface traps.¹¹ Future work will

compare time-resolved emission of QDs capped with different primary, secondary, and tertiary amines.

Water-Solubilized CdSe and ZnS(CdSe) with Thiol Compounds. A large change in the emission is observed when bare CdSe is solubilized with mercaptoacetic acid (MAA) (Figure 4). The faster decays and lower S/N (resulting in longer TCSPC collection times) correspond to the reduced quantum yield of these structures. It was previously reported that the photoexcitation of CdSe in a concentrated thiol-compound solution catalyzes the formation of disulfide bonds.²⁸ In this study, each CdSe nanocrystal is coated with many MAA groups. Thus, it is plausible that mercaptoacetic acid is an efficient hole acceptor of photoexcited CdSe, thereby breaking the Cd-S bond and reacting with a neighboring MAA group to form a disulfide bond. This process would quench the exciton emission and explain the reduced lifetimes for the water-soluble structures shown in Figure 4. Only a very small fraction of (CdSe)MAA would remain luminescent; in fact, when bare CdSe is solubilized with dihydrolipoic acid (DHLA), we find that this fraction is reduced to zero. The much smaller change in emission observed when ZnS-capped CdSe is solubilized with DHLA (Figure 5) is consistent with reduced access of the CdSe core to electron-transfer processes because of the ZnS cap.

The results shown in Figures 4 and 6 with adenine (6AP) and holotransferrin (HOLO) conjugated to (CdSe)MAA and (ZnS(CdSe))DHLA indicate that it is still possible to modulate the weak luminescence of these water-soluble structures. The oxidation potential of adenine is energetically close to the position of the valence band for luminescent green CdSe.⁴¹ This could explain the apparent additional quenching of peak-emitting 550 nm (CdSe)MAA and possible enhancement of peak-emitting 565 nm ZnS(CdSe). More studies with red and blue luminescent CdSe structures with adenine will be required to confirm this explanation. The protein holotransferrin was not expected to influence the emission dynamics, and no changes were observed with (CdSe)MAA.

Precipitation and Photoenhancement of MAA(CdSe) in Water. Finally, the photoenhancement of quantum dot emission has been previously studied on surfaces^{19,42} and in nonaqueous solvents.¹⁵ The former study⁴² indicated that the presence of water leads to an increase in luminescence intensity. The latter study¹⁵ speculated that surfactant molecules (possibly water) could stabilize surface trap states, thereby lengthening the trap state and hence emission lifetimes. Increased emission lifetimes are clearly observed with increased UV light exposure (Figure 5B), corresponding to an enhancement in steady-state emission (Figure 5A). This experiment is unique because it demonstrates CdSe photoenhancement in water. However, the results are complex because decay of the MAA coat occurs concurrently with prolonged UV exposure and photoenhancement. Stated differently, prolonged UV exposure causes two possible processes to occur with CdSe quantum dots water-solubilized with thiol compounds: first, decay of the thiol coat through the formation of disulfide bonds, which leads to CdSe precipitation, and second, possible coordination of surfactant molecules to the CdSe surface, which creates long-lived surface trap states and enhanced CdSe exciton emission. The first process helps the second process by increasing surface exposure to the environment.

Loss of solubility and aggregation of (CdSe)MAA over time was followed spectrophotometrically with the absorption spectra shown in the inset of Figure 5A. It is not until the CdSe begins to precipitate, as evidenced by the less clearly defined and

broadened absorption spectrum at 40 min, that photoenhancement occurs. This corresponds physically to significant decay of the MAA coat and a CdSe surface exposed to the aqueous environment. Because photoenhancement does not occur until precipitation starts, these results provide evidence for both of the above stated mechanisms. The blue shift in emission could be a result of a change in the ionic environment surrounding the nanocrystal¹⁵ and/or physical oxidation with dissolved O₂ of the exposed nanocrystal surface, resulting in desorption of SeO₂ and a smaller CdSe core. The photoenhancement effect appears to plateau around 150 min, though longer time scales of UV exposure were not measured.

It is noted that in a recent photoenhancement study with thiol-stabilized ZnSe in water the authors concluded that the surface was becoming S-enriched, leading to an increase in emission.¹⁶ It was speculated that a similar process was occurring with thiol-stabilized CdS quantum dots.⁴³ Although this may be a possibility with CdSe, this conclusion is difficult to rationalize with disulfide formation and precipitation of the quantum dots as well as the partial to complete quenching of the ZnS(CdSe) quantum dots when they are solubilized. We also observed that if the precipitated but photoenhanced CdSe is resuspended by adding additional MAA to the solution then the emission is readily quenched. In addition, in a previous study⁴⁴ we performed energy-dispersive X-ray spectroscopy (EDS) of the same QDs used in this work; all QDs and negligible amounts of S (<2 atom %) on the surface of QDs both before and after photooxidation were found for MAA-solubilized and adenine-conjugated QDs (data not shown; values <5 atom % are not quantitative).

Conclusions

The main goal of this research was to characterize the fluorescence emission spectra and decay curves of a single batch of CdSe quantum dots while varying the surrounding shells and solvents. Perhaps the most compared quantum dot structures have been between ZnS-capped and uncapped CdSe, mostly in inorganic solvents at room temperature.^{9,10} These results support previous conclusions that ZnS capping improves CdSe quantum yields by passivating surface traps. ZnS may affect deep and shallow trap states differently, possibly stabilizing shallow traps. Our key interest is with water-soluble quantum dots, where the effects of ZnS capping are more dramatic. Almost complete quenching occurs when CdSe is solubilized with thiol compounds, and this is reflected in the rapid decays observed in the time-resolved data. ZnS capping provides some minimal protection against quenching, although these thiol-solubilized structures are too unstable to be of long-term use. Although there are better techniques for stabilizing CdSe structures in water, few among them offer core accessibility. These results show that even with heavily quenched CdSe solubilized with mercaptoacetic acid it is still possible to modulate the emission using a hole acceptor such as adenine. Through careful choice of coating and solubilization agent, it should be possible to construct a nanocrystal-based sensor that operates in aqueous environments.

Acknowledgment. J.A.K. and J.L.N. acknowledge that this material is based upon work performed at the Jet Propulsion Laboratory, California Institute of Technology, supported by a contract with the National Aeronautics and Space Administration. S.E.B. is supported by the David and Lucile Packard Foundation. J.L.N. acknowledges salary support from the Canada Research Chairs. The TCSPC instrument was funded by NASA-JPL contract 1 250 277.

Supporting Information Available: Time-resolved spectra of QDs in H₂O versus PBS. This material is available free of charge via the Internet at <http://pubs.acs.org>.

References and Notes

- (1) Mattoussi, H.; Mauro, J. M.; Goldman, E. R.; Anderson, G. P.; Sundar, V. C.; Mikulec, F. V.; Bawendi, M. G. *J. Am. Chem. Soc.* **2000**, *122*, 12142.
- (2) Willard, D. M.; Carillo, L. L.; Jung, J.; Van Orden, A. *Nano Lett.* **2001**, *1*, 469.
- (3) Kowshik, M.; Deshmukh, N.; Vogel, W.; Urban, J.; Kulkarni, S. K.; Paknikar, K. M. *Biotechnol. Bioeng.* **2002**, *78*, 583.
- (4) Larson, D. R.; Zipfel, W. R.; Williams, R. M.; Clark, S. W.; Bruchez, M. P.; Wise, F. W.; Webb, W. W. *Science* **2003**, *300*, 1434.
- (5) Kloepfer, J. A.; Mielke, R. E.; Wong, M. S.; Nealon, K. H.; Stucky, G.; Nadeau, J. L. *Appl. Environ. Microbiol.* **2003**, *69*, 4205.
- (6) Murray, C. B.; Norris, D. J.; Bawendi, M. G. *J. Am. Chem. Soc.* **1993**, *115*, 8706.
- (7) Katari, J. E. B.; Colvin, V. L.; Alivisatos, A. P. *J. Phys. Chem.* **1994**, *98*, 4109.
- (8) Bawendi, M. G.; Carroll, P. J.; Wilson, W. L.; Brus, L. E. *J. Chem. Phys.* **1992**, *96*, 946.
- (9) Dabbousi, B. O.; RodriguezViejo, J.; Mikulec, F. V.; Heine, J. R.; Mattoussi, H.; Ober, R.; Jensen, K. F.; Bawendi, M. G. *J. Phys. Chem. B* **1997**, *101*, 9463.
- (10) Hines, M. A.; Guyot-Sionnest, P. *J. Phys. Chem.* **1996**, *100*, 468.
- (11) Talapin, D. V.; Rogach, A. L.; Kornowski, A.; Haase, M.; Weller, H. *Nano Lett.* **2001**, *1*, 207.
- (12) Burda, C.; Green, T. C.; Link, S.; El-Sayed, M. A. *J. Phys. Chem. B* **1999**, *103*, 1783.
- (13) Sirota, M.; Minkin, E.; Lifshitz, E.; Hensel, V.; Lahav, M. *J. Phys. Chem. B* **2001**, *105*, 6792.
- (14) Shim, M.; Wang, C. J.; Guyot-Sionnest, P. *J. Phys. Chem. B* **2001**, *105*, 2369.
- (15) Jones, M.; Nedeljkovic, J.; Ellingson, R. J.; Nozik, A. J.; Rumbles, G. *J. Phys. Chem. B* **2003**, *107*, 11346.
- (16) Shavel, A.; Gaponik, N.; Eychmuller, A. *J. Phys. Chem. B* **2004**, *108*, 5905.
- (17) Hess, B. C.; Okhrimenko, I. G.; Davis, R. C.; Stevens, B. C.; Schulzke, Q. A.; Wright, K. C.; Bass, C. D.; Evans, C. D.; Summers, S. L. *Phys. Rev. Lett.* **2001**, *86*, 3132.
- (18) Underwood, D. F.; Kippeny, T.; Rosenthal, S. J. *J. Phys. Chem. B* **2001**, *105*, 436.
- (19) Sark, W. G. J. H. M. v.; Frederix, P. L. T. M.; Heuvel, D. J. V. d.; Gerritsen, H. C.; Bol, A. A.; Lingen, J. N. J. v.; Donega, C. d. M.; Meijerink, A. *J. Phys. Chem. B* **2001**, *105*, 8281.
- (20) Demchick, P.; Koch, A. L. *J. Bacteriol.* **1996**, *178*, 768.
- (21) Wang, H. W.; Chen, Y.; Yang, H.; Chen, X.; Duan, M. X.; Tai, P. C.; Sui, S. F. *Proc. Natl. Acad. Sci. U.S.A.* **2003**, *100*, 4221.
- (22) Liu, G.; Li, D.; Pasumathy, M. K.; Kowalczyk, T. H.; Gedeon, C. R.; Hyatt, S. L.; Payne, J. M.; Miller, T. J.; Brunovskis, P.; Fink, T. L.; Muhammad, O.; Moen, R. C.; Hanson, R. W.; Cooper, M. J. *J. Biol. Chem.* **2003**, *278*, 32578.
- (23) Chan, W. C.; Nie, S. *Science* **1998**, *281*, 2016.
- (24) Dubertret, B.; Skourides, P.; Norris, D. J.; Noireaux, V.; Brivanlou, A. H.; Libchaber, A. *Science* **2002**, *298*, 1759.
- (25) Kloepfer, J. A.; Cohen, N.; Nadeau, J. L. *J. Phys. Chem. B* **2004**, *108*, 17042.
- (26) Rogach, A. L.; Kornowski, A.; Gao, M. Y.; Eychmuller, A.; Weller, H. *J. Phys. Chem. B* **1999**, *103*, 3065.
- (27) Rogach, A. L.; Nagesha, D.; Ostrander, J. W.; Giersig, M.; Kotov, N. A. *Chem. Mater.* **2000**, *12*, 2676.
- (28) Aldana, J.; Wang, Y. A.; Peng, X. G. *J. Am. Chem. Soc.* **2001**, *123*, 8844.
- (29) Wong, M. S.; Stucky, G. D. *Abstr. Pap. Am. Chem. Soc.* **2001**, *221*, U572.
- (30) Zhang, C. X.; O'Brien, S.; Balogh, L. *J. Am. Chem. Soc. B* **2002**, *106*, 10316.
- (31) Hermanson, G. T. *Bioconjugate Techniques*; Academic Press: San Diego, CA, 1996.
- (32) Kumar, A.; Negi, D. P. S. *J. Colloid Interface Sci.* **2001**, *238*, 310.
- (33) Schmelz, O.; Mews, A.; Basche, T.; Herrmann, A.; Mullen, K. *Langmuir* **2001**, *17*, 2861.
- (34) Magde, D.; Rojas, G. E.; Seybold, P. G. *Photochem. Photobiol.* **1999**, *70*, 737.
- (35) Oneil, M.; Marohn, J.; McLendon, G. *J. Phys. Chem.* **1990**, *94*, 4356.

- (36) Wu, X.; Liu, H.; Liu, J.; Haley, K. N.; Treadway, J. A.; Larson, J. P.; Ge, N.; Peale, F.; Bruchez, M. P. *Nat. Biotechnol.* **2003**, *21*, 41.
- (37) Chikan, V.; Kelley, D. F. *J. Chem. Phys.* **2002**, *117*, 8944.
- (38) Burda, C.; Link, S.; Mohamed, M.; El-Sayed, M. *J. Phys. Chem. B* **2001**, *105*, 12286.
- (39) Donega, C. M.; Hickey, S. G.; Wuister, S. F.; Vanmaekelbergh, D.; Meijerink, A. *J. Phys. Chem. B* **2003**, *107*, 489.
- (40) Qu, L.; Peng, Z. A.; Peng, X. *Nano Lett.* **2001**, *1*, 333.
- (41) Goodwin, T. W. *The Biochemistry of the Carotenoids*, 2nd ed.; Chapman and Hall: London, 1980; Vol. 1.
- (42) Cordero, S. R.; Carson, P. J.; Estabrook, R. A.; Strouse, G. F.; Buratto, S. K. *J. Phys. Chem. B* **2000**, *104*, 12137.
- (43) Dollefeld, H.; Hoppe, K.; Kolny, J.; Schilling, K.; Weller, H.; Eychmuller, A. *Phys. Chem. Chem. Phys.* **2002**, *4*, 4747.
- (44) Kloepper, J. A.; Mielke, R. E.; Nadeau, J. L. *Appl. Environ. Microbiol.* **2005**, May, 71.